THE GEOPHYSICAL INSTITUTE OF ISRAEL המכון הגיאופיסי לישראל
6 HABAAL SHEM TOV ST. LOD, ISRAEL 7128906 הבעש"ט 6, לוד, ישראל
P.O.B 182, 7110101 TEL: +972-8-9785888 FAX: +972-8-9208811 www.gii.co.il

GII Internal Report No 030/792/14 **November 2014**

AUTOMATIC LOCATION AND MOMENT MAGNITUDE Mm ESTIMATION USING TRIGGERED SEISMIC TRACES OF THE ISRAEL SEISMIC NETWORK

Dr. Vladimir Pinsky

Seismological Department

of the Geophysical Institute of Israel

Contents

Table of Figures

List of Tables

INTRODUCTION

The automatic location procedure "**autoloc_gii**" now used in the Seismological Department of the Geophysical Institute of Israel has two versions: real-time "**rautoloc_gii**" (Polozov & Pinsky, 2008) and trigger based "**tautoloc_gii**", both developed according approach of Pinsky & Horiuchi, 2008. The first one provides detection and location based on the current waveforms and the initial result (based on 6 first stations picks) is ready within 10 - 20 sec after the first P-wave detection. The last one utilizes the 2 and the 5 minute records extracted from the ring-buffer after the event is triggered by the conventional STA/LTA procedure. The **rautoloc_gii** is recommended for the fast "first glance" report about earthquake epicenter and magnitude. The **tautoloc_gii** is a more thorough elaboration of the earthquake parameters, accounting for the possible scenario of multiple events as well. The **tautoloc_gii** was recently upgraded for the more accurate and reliable location. This report targets to analyze the performance of the upgraded tautoloc_gii procedure with a new addition block developed for **automatic estimation** of the spectral moment magnitudes Mm. The magnitudes are based on the displacement spectra of the S and the P waves: M_{ms} and M_{mP} respectively. The Mms and the Mwp estimates follows Shapira& Hofstetter, 1993 and Ataev & Hofsteter, 2014 formulations with an attempt to use a broader magnitude and distance range than those, which originally have been used. Therefore, it should be understood that a larger scatter of the estimates than those originally reported are possible.

METHOD

Automatic Location procedure tautoloc_gii in general remains untouched version of January 2012. However, several innovations concerning trace filtering, (filtrec2.f), teleseismic location (see teletest4.f) and local location procedure (beamrdet5c.f) have been introduced and can be found in the new procedure "reglocatorJan2012n.s" in the archive sysop@199.71.138.211/data/backup/EXPORTAPRIL2010.

Automatic Magnitude estimation is provided by the grid-search least-squares fitting of a trapeze function $y=y(f, A, f_c)$:

$$y = \begin{cases} A, & f < f_c; \\ A - 2(f - f_c), & f \geq f_c \end{cases}$$

to the logarithm of smoothed displacement spectra *D*(*f*) (see Figure 1.), (a routine manually performed by analysts for example, using JSTAR utility), where *f=i df* – discrete frequency: i=1, ...N. As the result for each of the phases at a trace we get A_0, f_c as minimum of function *S(A, f):*

$$S = \sum [(D(f) - y(f, A, fc))]^2$$

Magnitude was estimated for the Trillium Compact stations (TC) only, which are now the majority of the ISN network. For magnitude Mm_P and Mm_S estimation I utilized the seismic moment – spectral amplitude A_0 –distance R relationships for P and S waves derived in Ataeva & Hofstetter, 2014 and Shapira & Hofstetter, 1993 respectively. Note that these relationships have been obtained for the magnitude: 2.7 < Md < 5.6 and 3. < ML < 6.7 ranges and distance range of 8 < R < 550 km , which differ from the data range used for the current analyses (see the following section), where all triggered data have been used up to 700 km distance range to the farthest station. The target was to characterize the equations in a broader data range and an attempt to expand their applicability in automatic manner.

DATA

We have taken from the “seisdb” database (server 199.71.138.242) all the triggered waveforms of earthquakes, within the rectangle: 32 º E – 38 º E; 27 º N – 35 º N; that gave us a list of 203 events for the period 01.01.2013 – 01.09.2014 (see Figure 2). During the period the network was presented by the 32 stations listed with main parameters in the Table 1 and shown in Figure 1 jointly with the event's epicenters. The poles-and-zeros information for the Trillium Compact stations (TC) only was used for the instrument response removal and the event magnitude estimation.

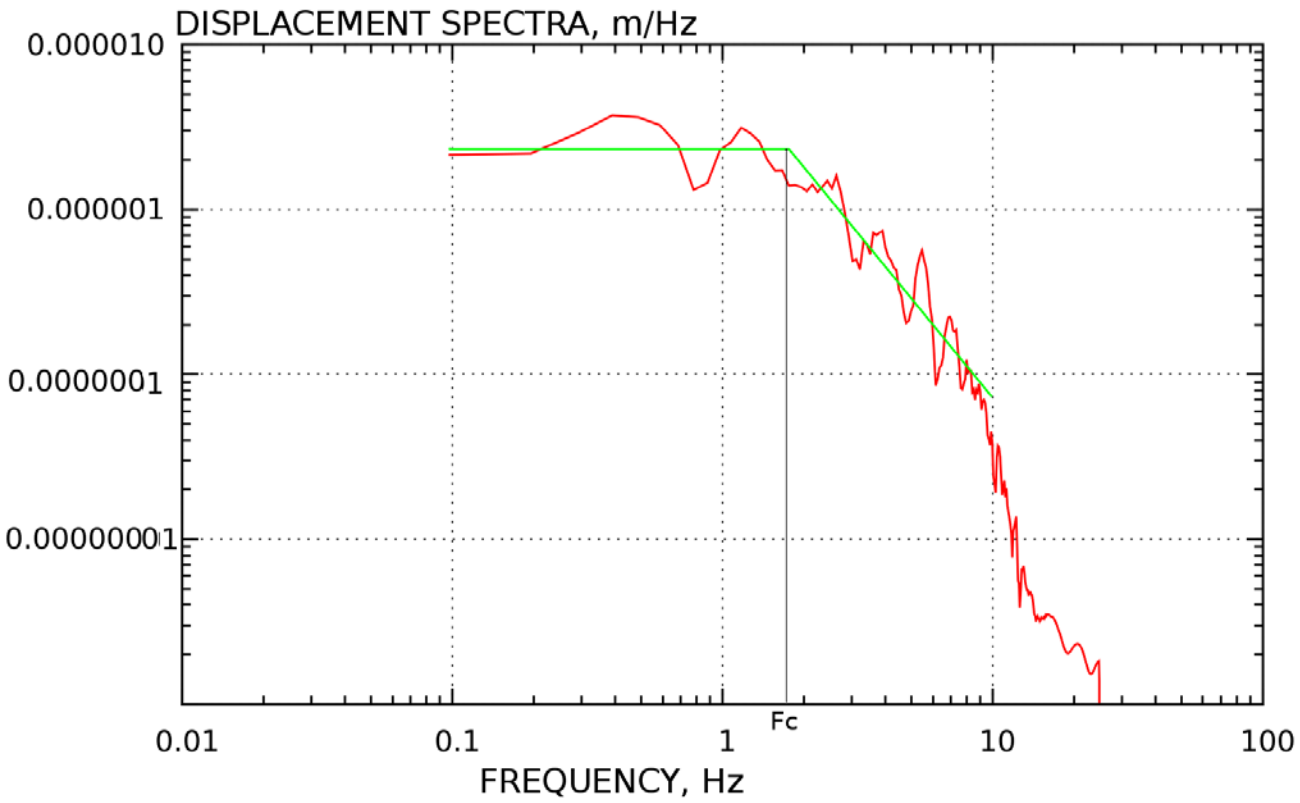

Figure 1. Displacement spectra and moment magnitude determination using "trapeze approximation"

RESULTS

Below are the results of automatic processing of the waveforms according the list. The

LOCATION RESULTS

Figure 2. demonstrates epicenter distribution and location accuracy of the tautoloc_gii procedure for the 203 events by using different colors of the circles depending on distance between automatic and manual solutions. The location error analysis is summarized in Figure 2 where we depict percent of event located with error of epicenter location less than R (empirical probability distribution function). The empirical distribution of the error is depicted for two regions: the whole region, mentioned above and the smaller region of local events, taken into the frame in Figure 1. From Figures 1 and 2 it is seen that for the inner area the automatic location is almost perfect giving error < 10 km for 95% of events. whilst for the whole area it is only 40% of events. Among the events with err > 10 km the essential

majority lie out of the network coverage: mostly to the North and to the South of the network. (see Figure 1). The main reasons for large errors: large station gap, wrong velocity model, bad SNR at P and/or S phase arrivals or small number of channels with high SNR, and multiple events. Malfunctioning of the acquisition system might be also the cause of erroneous location. Most of discrepancies between automatic and manual solutions are for the Cyprus region and the adjacent area. This strange fact needs additional investigation.

Table 1. Station parameters used in the study.

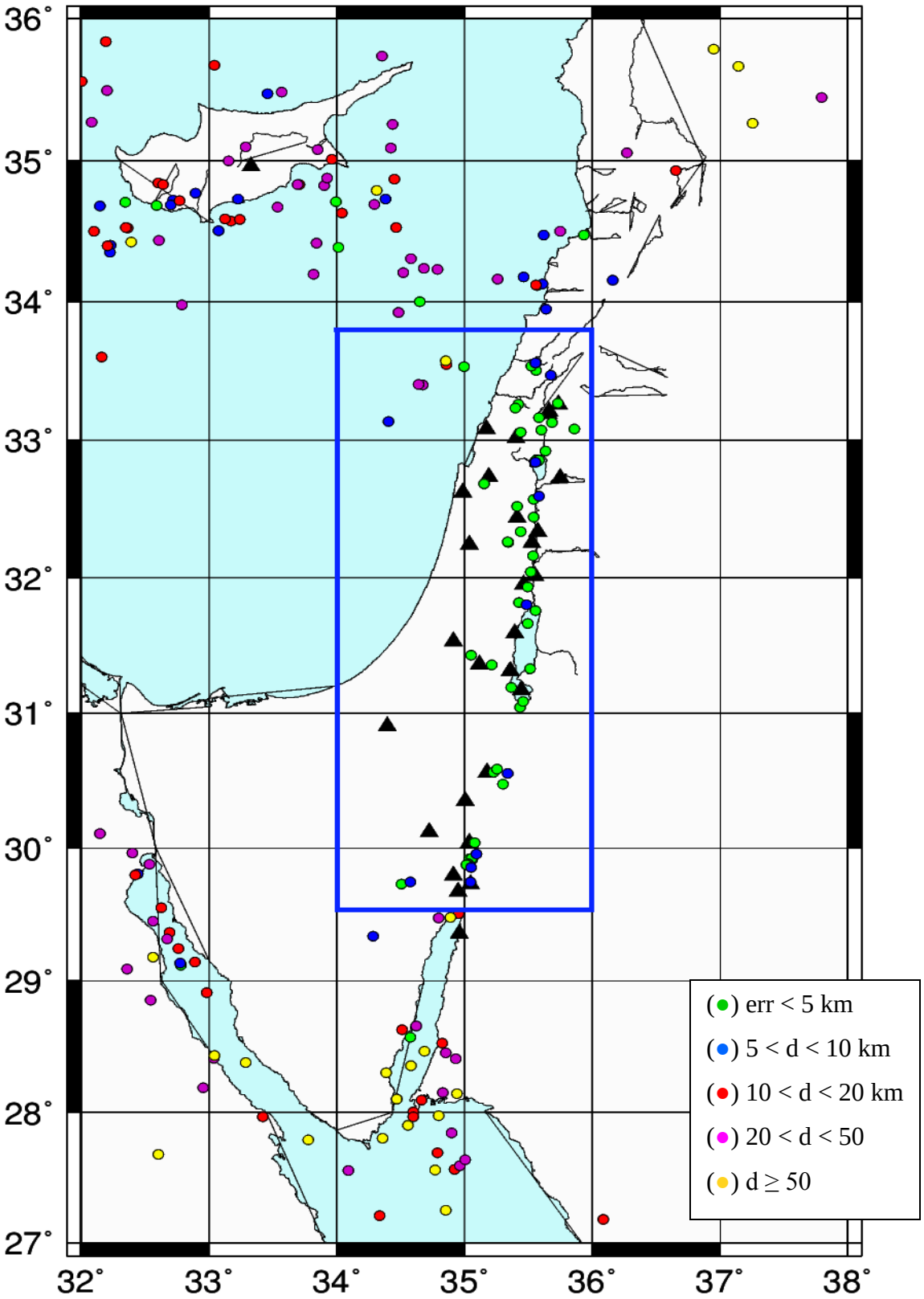

Table 2. Automatic Location results for the 203 triggered events M≥2.

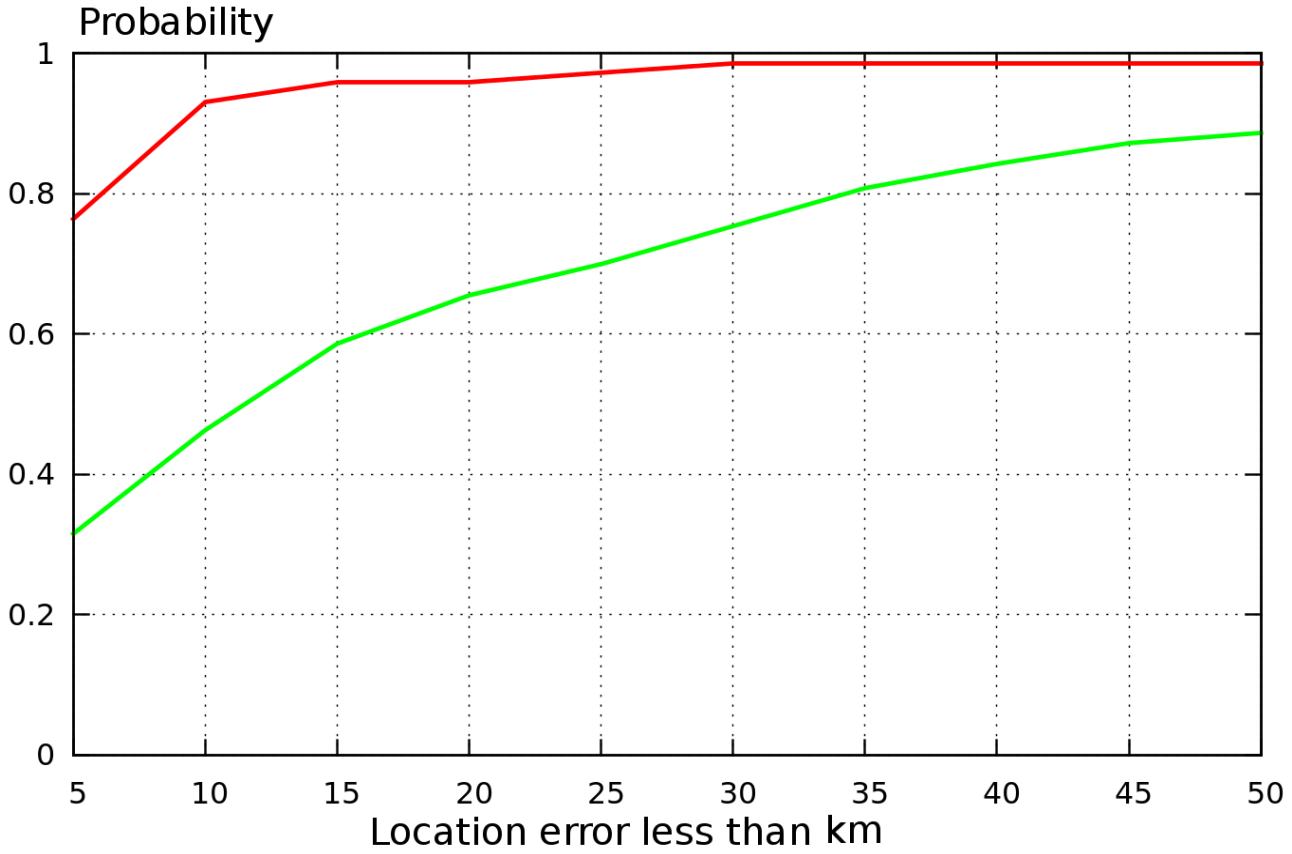

Figure 2. Empirical probability distribution function P{err < R} for the area 34 º E – 36 º E; 29.5 º N – 33.8 º N -green and 32 º E – 38 º E; 27 º N – 35 º N -red, where location error is the distance between the manual and automatic epicenter solutions.

MAGNITUDE ESTIMATION RESULTS

Magnitudes Mms and Mmp have been estimated first for the fixed 10 seconds after automatic on-set of the S-wave and fixed 5 seconds of the P-wave respectively. Then the variable time windows have been used (see below). Only stations participating in location and having SNR > 2 have been taken for the magnitude estimation. For the 171 events with determined Md from the marked area 34 º E – 36 º E; 29.5 º N – 33.8 º N we have got the following statistics: |Md - Mms| < 0.5 for 73% and for 136 events with |Md - Mmp| < 0.5 for 43% of events. Figure 4. shows histograms of deviation of magnitude estimates Mms and Mmp from manually estimated duration magnitude Md. If the first is symmetric the least is biased towards ~ 0.5 unit larger values. For the 65 events with determined Md from the sub-region mentioned above we have got the following statistics: |Md - Mms| < 0.5 for 89%

and for 60 events with |Md - Mmp| < 0.5 for 33% of events. Figure 4. shows histograms of deviation of magnitude estimates Mms and Mmp from manually estimated duration magnitude Md. If the first is symmetric the least is biased towards ~ 0.5 unit larger values.

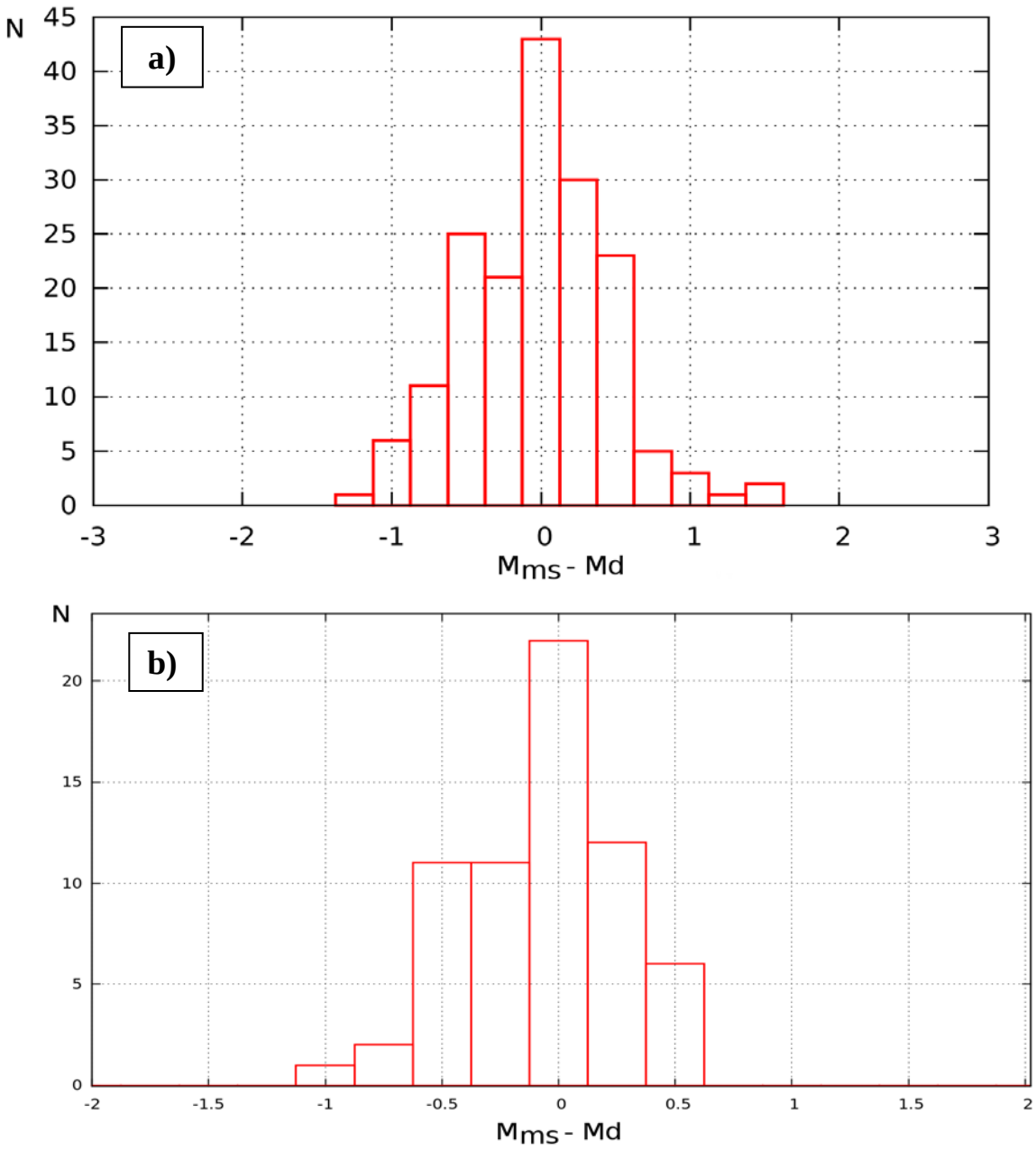

Figure 3. Histogram of deviation (a) Mms and (b) Mmp from duration magnitude Md for all the area.

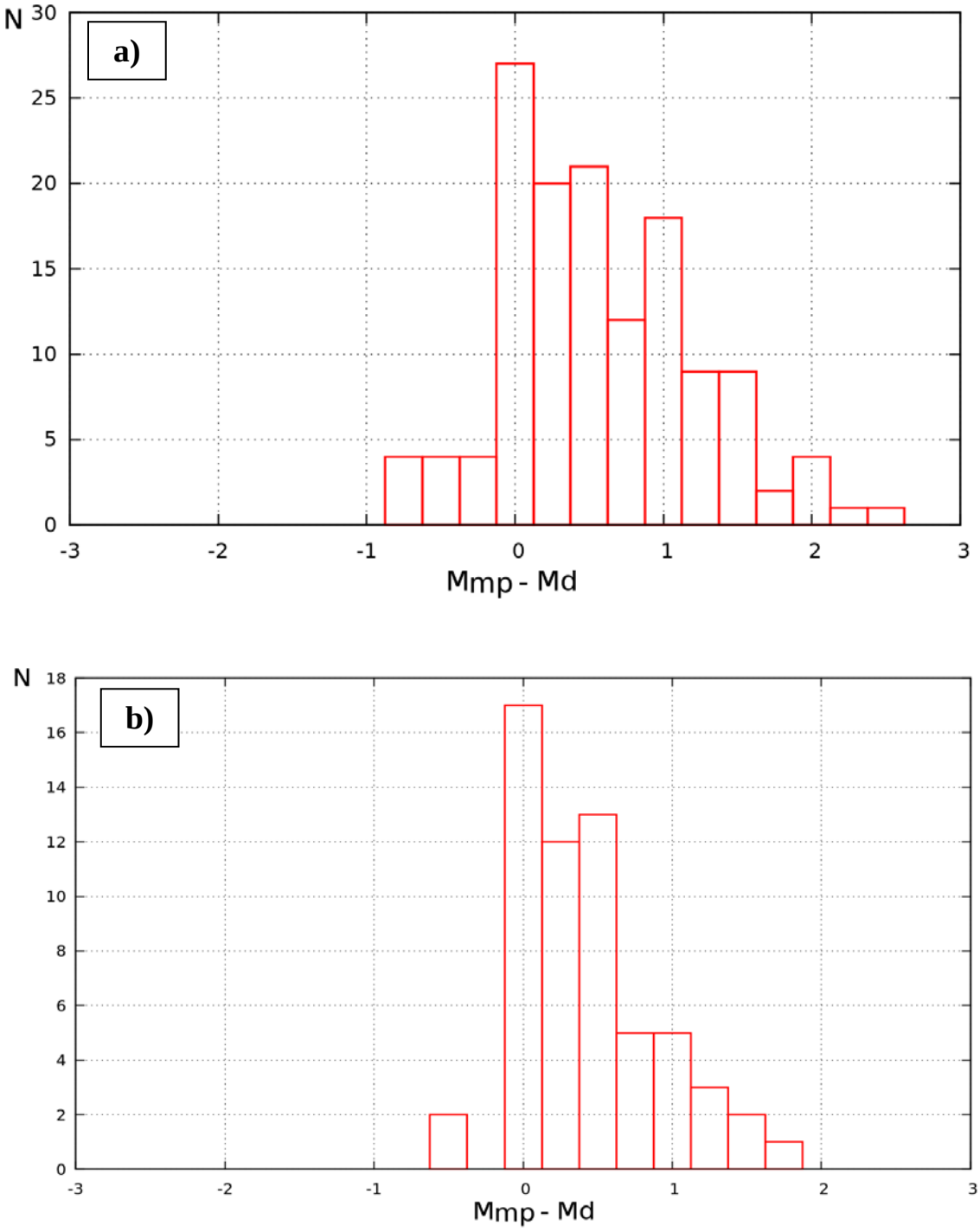

Figure 4. Histogram of deviation (a) Mms and (b) Mmp from duration magnitude Md for the sub-region area 34 º E – 36 º E; 29.5 º N – 33.8 º N

For improving the result of automatic magnitude estimation we tried using variable time windows for P and S waves. For P wave this would might help to avoid entering of S waves into the P

wave window. For S waves variable time window allows to account for the energy of S and Lg, Rg waves. As for P waves we choose time-windows due to the equation:

$$W_p = \begin{cases} 2\,\text{sec}, R < 100\ km \\ 3\,\text{sec},\ \ 100 < R\ \le 200\ km \\ 3 + \dfrac{R - 200}{100}\,\text{sec}\ \ R > 200\ km \end{cases}$$

And for the S-waves

$$W_s = R\left(\frac{1}{V_s} - \frac{1}{V_p}\right) + 20/F_0,$$

with $V_p = 6\frac{km}{s}, V_s = 3\frac{km}{s}$

Figure 6 and 7 show distribution of automatic magnitudes for P and S waves respectively versus Md. The green regression lines shown in the figures prompt correction for the estimates that might improve the result. As seen from the histograms in Figures 8 (for all 203 events) and 9 for sub-region 73 events the time varying windows didn't essentially improve distribution of the magnitude estimates. However, the magnitude transformation due to the regression lines for P waves

$M_{mp} = (\widehat{M}_{mp} - 1.5)/0.6$,

and for S waves:

$M_{ms} = (\widehat{M}_{ms} - 1.1)/0.6$

helped to make distribution more symmetric and concentrated around Md value.

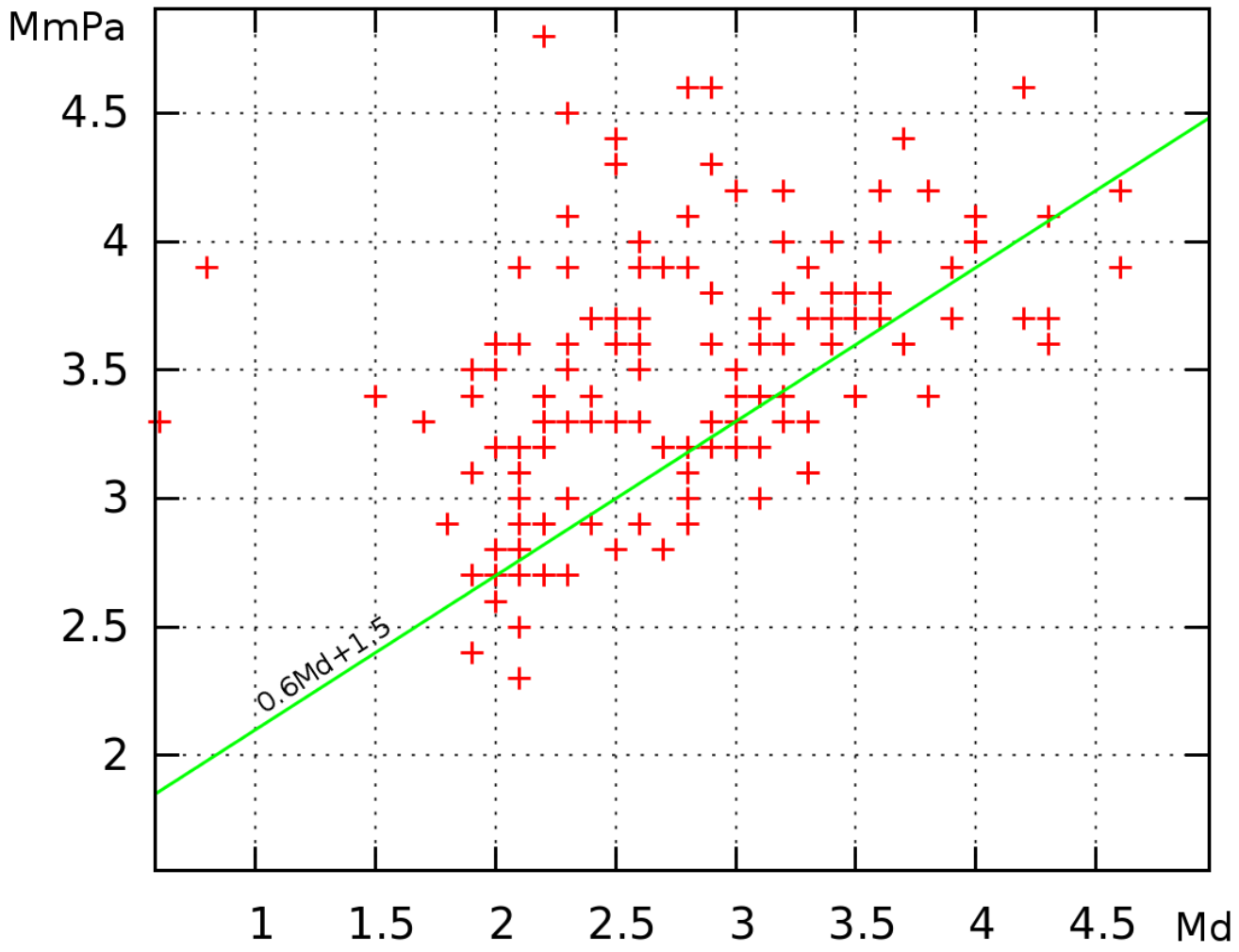

Figure 5. Automatic P wave magnitude MmP is shown versus Md for all 203 events. The proposed regression line is shown by green. Note that the magnitude range here is different from that of Ataeva & Hofstetter, 2014, including lower magnitudes and thus less stable. However, in the range 3.25 < Md < 4.6 the data scatter looks much more reduced.

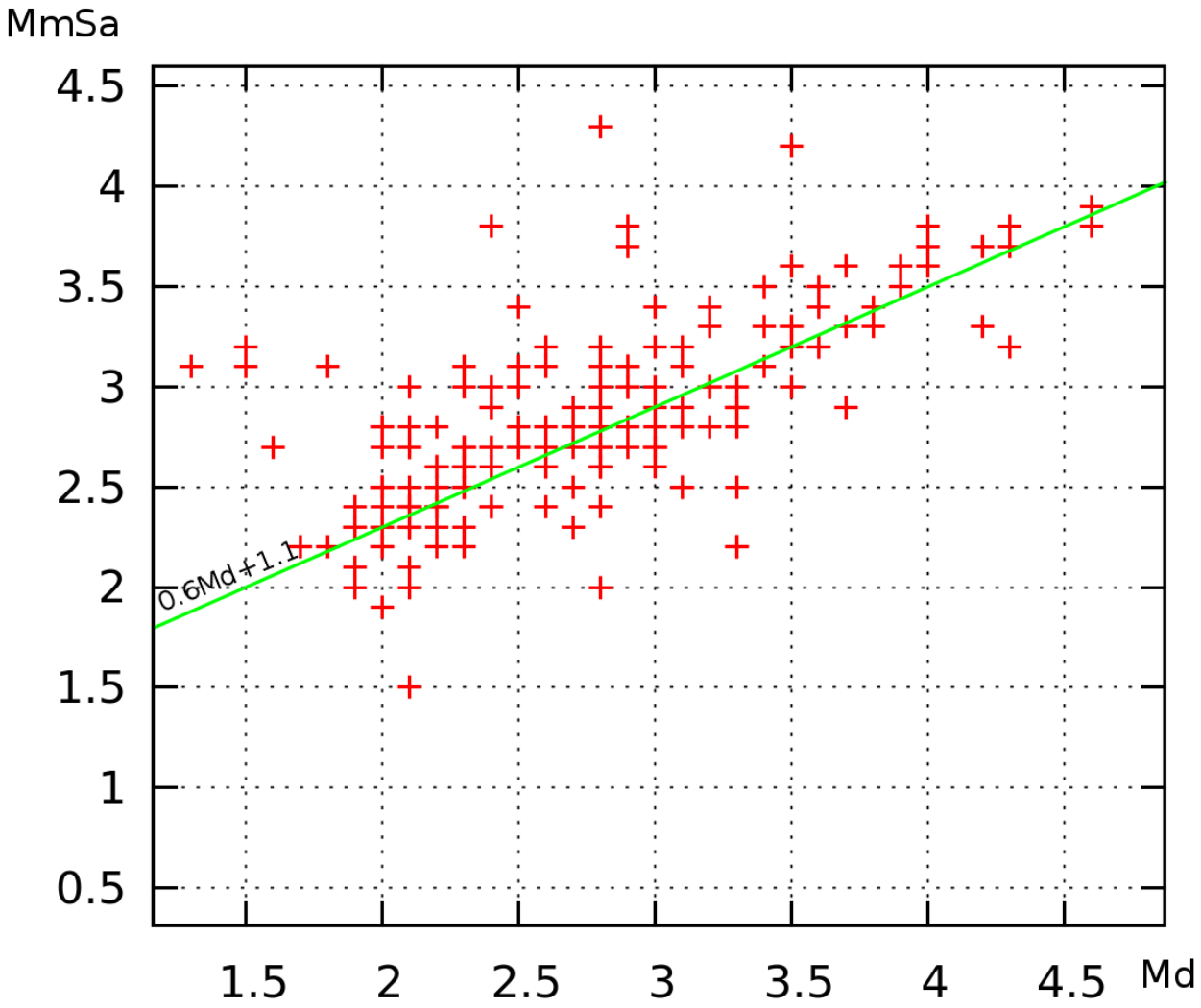

Figure 6. Automatic S wave magnitude MmS is shown versus Md for all 203 events. The proposed regression line is shown by green.

a)

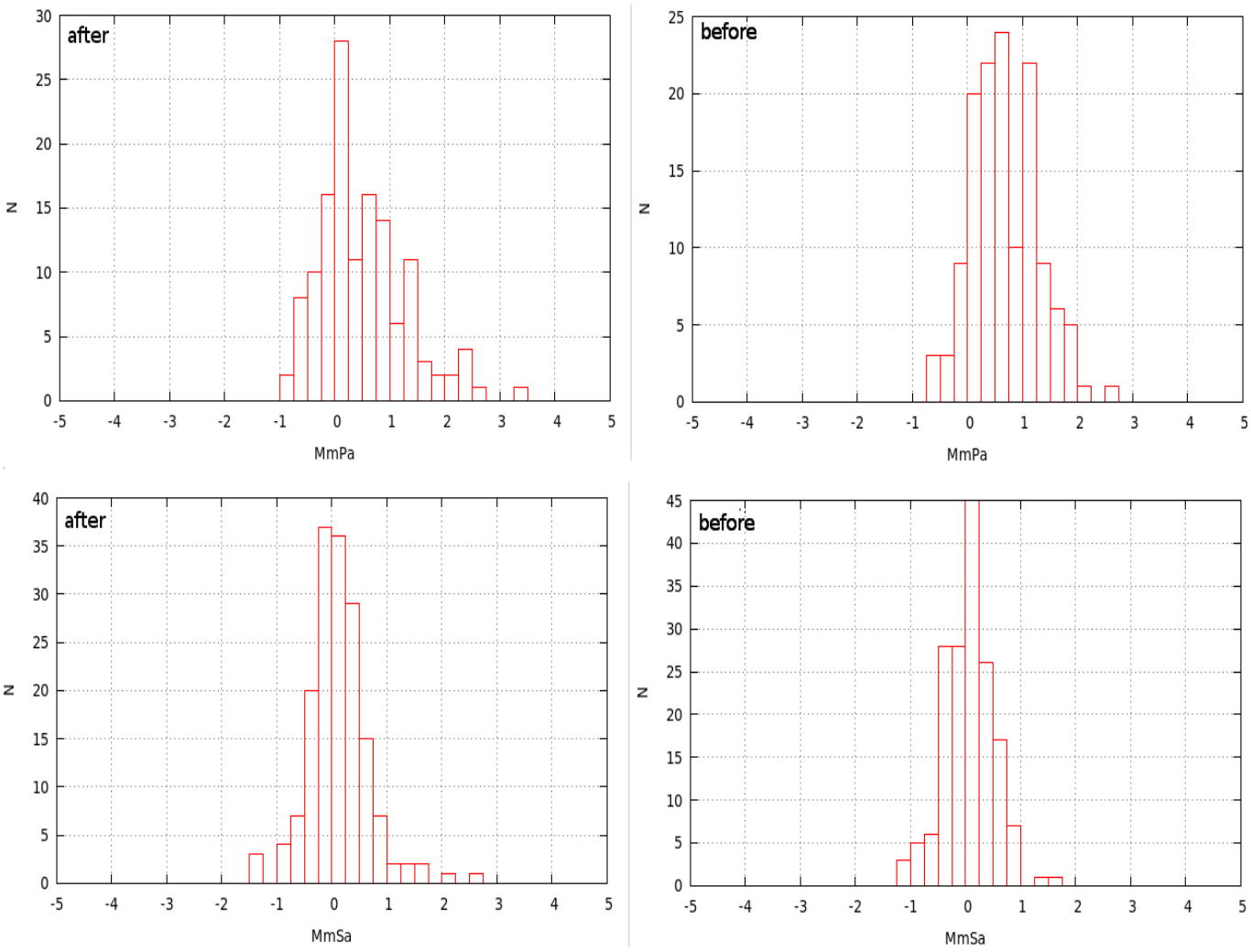

Figure 7. All 203 events histograms of automatic magnitude distribution for P (a) and S (b) waves for the variable time windows before and after proposed transformation

.

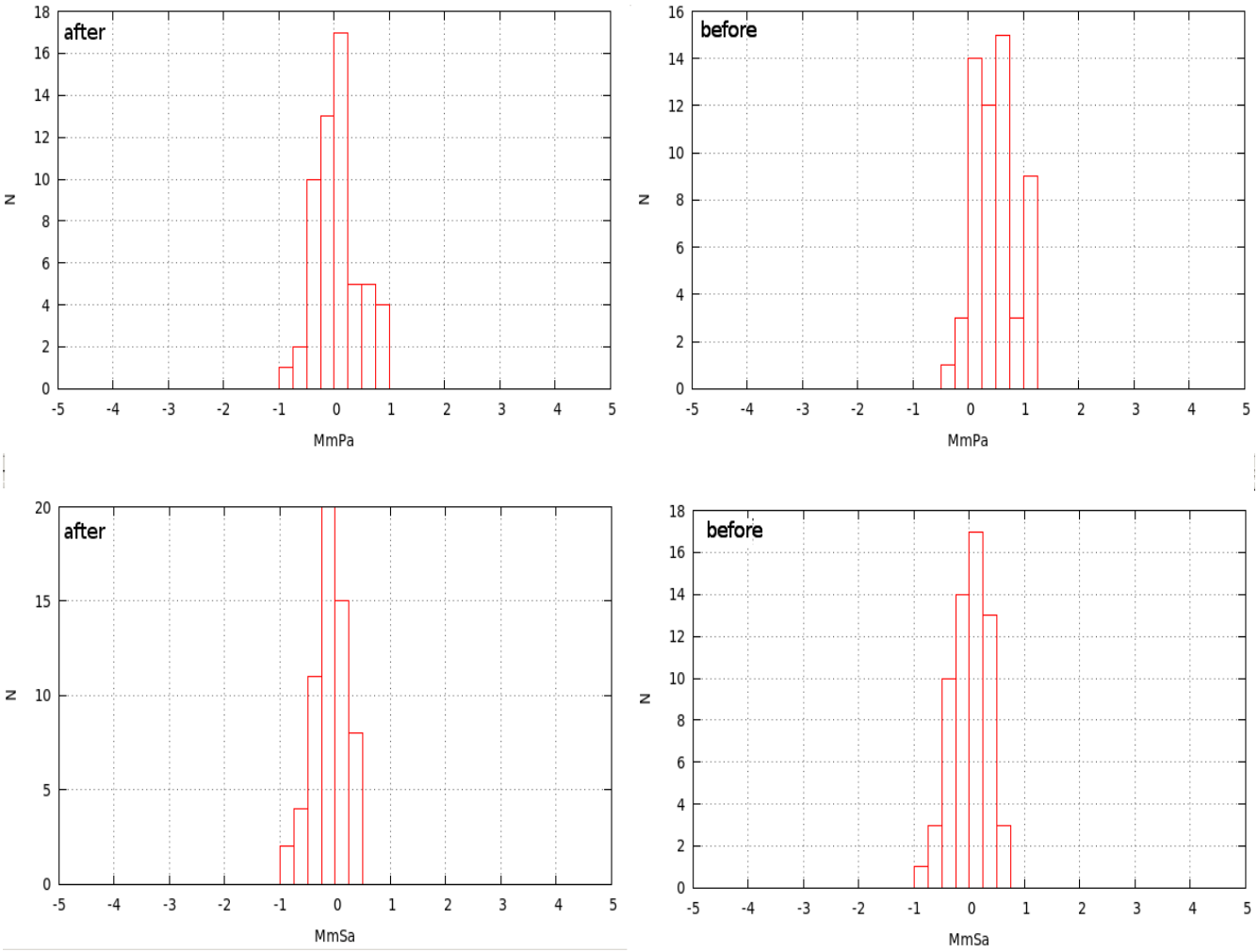

Figure 8. Sub-regional (mentioned above) events histograms of automatic magnitude distribution for P and S waves for the variable time windows before and after proposed transformation

CONCLUSIONS

The upgraded tautoloc procedure allows accurate and reliable epicenter estimation with error less than 10 km for 95 percent of events for local events in the region between 29.5 N – 33.75 N and 34 E – 36 E including all territory of Israel and partially Lebanon, Syria, Jordan, Egypt and Saudi Arabia as well as the corresponding part of the Mediterranean sea. However, for the outer events the location is much poorer, which is explained by the bad constrain of the network, wrong velocity model and bad signa-to-noise ratio for small events.

New automatic magnitude based on Mmp and Mms displacement spectra estimation showed satisfactory performance, as compared to the routine manual Md magnitude. However, the outliers are

probable for both Mws and Mwp. The Mms magnitude estimate looks more reliable at the whole region and at low magnitudes due to better signal-to-noise ratio for S-waves than for P-waves. For further improvement of the procedure a more detailed analyses is required including manual determination of the spectral Mwp and Mws magnitudes and a larger data-base of events.

REFERENCES

Ataev G., A. Hofstetter, (2014). Determination of source parameters for local and regional earthquakes in Israel (in Review of Journal of Seismology).

Pinsky V. and S. Horiuchi, 2008. Pinsky V., S. Horiuchi, 2009. Hypocenter location of mixed events in real-time processing systems. J. seismology. V 14. DOI 10.1007/s10950-009-9152-4.

Polozov A., V. Pinsky. 2008. New software for seismic network and array data processing and joint seismological database. Annual report for the ministry of National Infrastructures, Earth Sciences Research Administration GII Report: 546/404/08.

Shapira A., A. Hofstetter (1993). Source parameters and scaling relationships of earthquakes in Israel. Tectonophysics, v. 217 pp. 217-226. DOI: 10.1016/0040-1951(93)90005-5